The Eurasia Proceedings of Science, Technology, Engineering & Mathematics (EPSTEM)
ISSN: 2602-3199

The Eurasia Proceedings of Science, Technology, Engineering & Mathematics (EPSTEM), 2023

Volume 26, Pages 156-165

IConTES 2023: International Conference on Technology, Engineering and Science

Examining the Performance of the Heat Exchanger in a Heat Pump Clothes Dryer

Fazıl Erinc Yavuz
Haier Europe – Renta Elektrikli Ev Aletleri San ve Dıs Tic. Ltd. Sti

Vasif Can Yıldıran
Haier Europe – Renta Elektrikli Ev Aletleri San ve Dıs Tic. Ltd. Sti

Sebastian George Colleoni
Haier Europe

Abstract: The performance of the newly designed fin and tube heat exchanger placed within the heat pump tumble dryer (HPTD) has been numerically and experimentally investigated. A new heat exchanger (HX) has one inlet and one outlet for the refrigerant side. However, after insertion into the evaporator, the flow splits into two different branches and reaches a lower pressure than the standard one. Also, due to the separation more tube bundles can be fitted in the same amount of volume. Due to increased tube bundles, total heat transfer is increased. This behavior can be seen with numerical and experimental results. Also, the fin structures on the heat exchanger were removed from the model to avoid increasing the solution grid density. In this region, it was defined as a porous structure to accommodate the pressure drop. To solve the problem, the program called ANSYS-FLUENT was utilized to solve the problem, and the PISO algorithm was employed to solve the pressure-velocity pair. While air at a specified temperature was passed around the exchanger, water was circulated on the inner surface instead of the refrigerant gas to observe the temperature change.

Keywords: CFD, Tumble dryer, Heat exchanger, Evaporator, Porous media, Heat transfer

Introduction

Energy consumption of household appliances has a big impact on climate, water usage and resource consumption because of their electricity usage. To reduce these consumptions academicians and engineers are working tirelessly. Due to increasing number of tumble dryers is also impact on the total consumption. In this study, effect of newly developed heat exchanger is investigated as an evaporator in the heat pump tumble dryer.

Heat exchangers widely investigated in literature and finding a higher capacity in same volume is essential for household appliances, but increasing the capacity is not always comes with the better results, because of the flow resistance on the air side or some other adverse effects.

In a study that conducted conjugated heat transfer simulation in a fin and tube heat exchanger, they indicate that, increasing turbulence effect have a positive effect on heat transfer rate due to the increase in the heat exchange coefficient as expected with an increased power needs on the air flow side (Välikangas & Karvinen, 2018). On another study, frost formation was investigated numerically and experimentally, they have used porous media assumption and they have found frost layer formation has significant effect on heat transfer between air and fins (Lenic et al., 2009). Beside Lenic and his team study, in the literature there are lots of frost layer formation study with porous media assumption (O'Neal & Tree, 1984; Sami & Duong, 1989; Lee et al., 2003; Yao et al., 2004).

The other studies, has widely investigated the arrangement of refrigerant circuits, configuration of fins and tubes and operating conditions (Liu et al., 2004; Lu et al., 2011). In other study, experimental study has been conducted and compared with the well-known correlations such as Dittus-Boelter, Blasius, Gnielinski and Haaland with maximum difference 7.5% (Siddique & Alhazmy, 2008). In our study, refrigerant circuit on fin and tube heat exchanger has been taken from CAD model and fins are modelled as a porous media for a comparison test.

Method

This study consists of three phases. First one is design phase, for three-dimensional CAD model Creo Parametric has been used. Pipe designs were created according to the design constraints of the current plastic basement, also inlet and outlet pipe location were decided according to the same plastic part. Second phase can be summarized at CFD studies, in this phase capacity comparison and air flow distribution were conducted. For this phase commercial CFD solver ANSYS Fluent had been used.

Third phase can be called as prototype creation and experimental study. For prototype phase, producibility of the design were investigated with the supplier of relevant part. Afterwards, tumble dryer was built with the prototype evaporators and tests were conducted. In first test, current configuration and new configuration had been tested under same ambient conditions and comparison were conducted. In second test energy consumption test had been conducted according to relevant standard (IEC 61121 – Tumble Dryers for Household Use-Methods for Measuring the Performance).

Design Phase

At the beginning of the study, the investigation on current evaporator was conducted which is shown on left side of Figure 1. Green arrows show the air flow and blue lines shows the refrigerant flow. Solid lines show the right-side u-bends of the evaporator while the dashed lines show the left-side u-bends. First idea is adding more pipes to the evaporator to enhance heat transfer capacity. However, due to the mechanical and producibility restrictions such as minimum bending radius of Al or Cu pipe and geometrical constraints this idea was cancelled. Second idea was splitting the refrigerant flow into two different branches at the entrance of the evaporator and with that split dimension between the pipes (h) can be reduced and more pipes can be added into the system. After the investigation of couple of design parameters, final heat exchanger design was created, and the figure of refrigerant flow is shown on the right side of Figure 1.

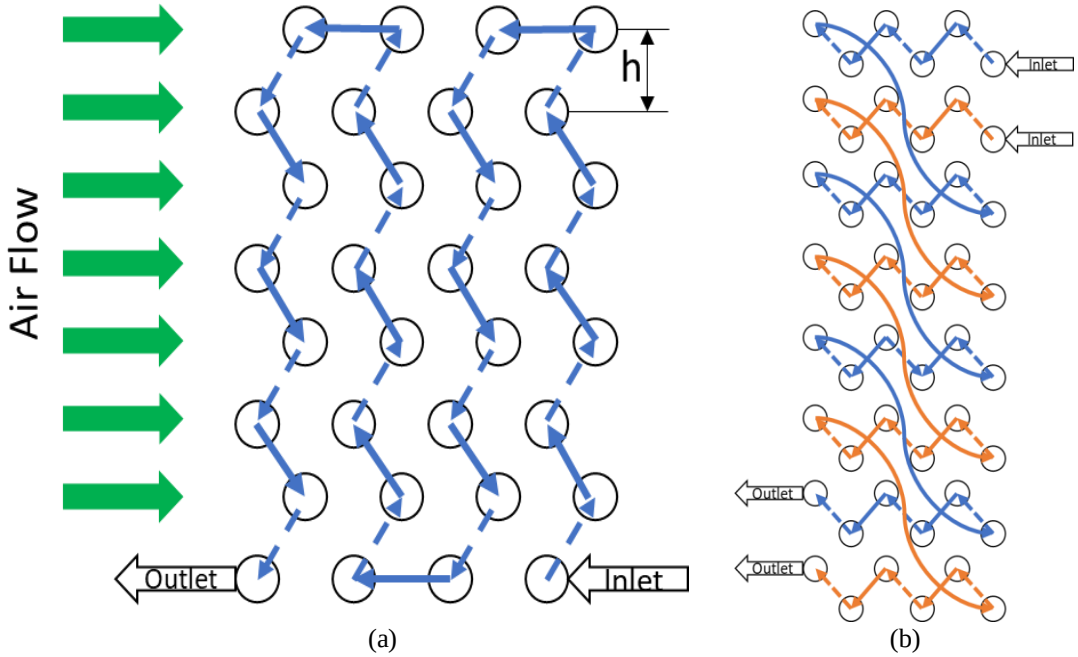

(a) (b)

Figure 1. Heat exchanger refrigerant circuit comparison a) Current b) New design

Simulation Phase

Three-dimensional model of the current and new evaporator placed in the cavity and two analyses were conducted under same input and boundary conditions. ANSYS Fluent commercial software was used as a solver and solution had been conducted under steady-state conditions. Due to the high mesh requirement, fins are modelled as a porous medium. In an earlier study, evaporator porous zone has been modeled and the constants for the porous zone has achieved and validated with the pressure difference test that was conducted by our team. In Figure 2 pressure drop values at different velocities has given.

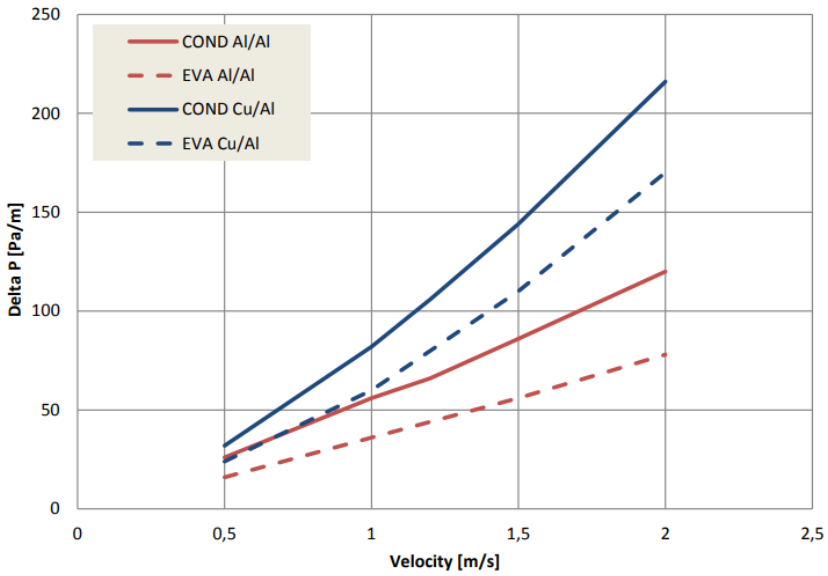

Figure 2. Pressure drop on the condenser and evaporator for different air velocity values

The cavity was generated in ANSYS SpaceClaim and the solution geometry is shared in Figure 3. To solve the problem mesh generation is needed. The mesh is generated on Fluent Mesh software with approximately 6.5 million cells. The mesh visual is shared in Figure 4. Five different meshes were generated in Fluent Mesh and analysis were conducted for the mesh independency study, which is shared in Figure 5. The difference between tests and analyses were found approximately 0.3%. The rest of the analyses were conducted under same mesh properties.

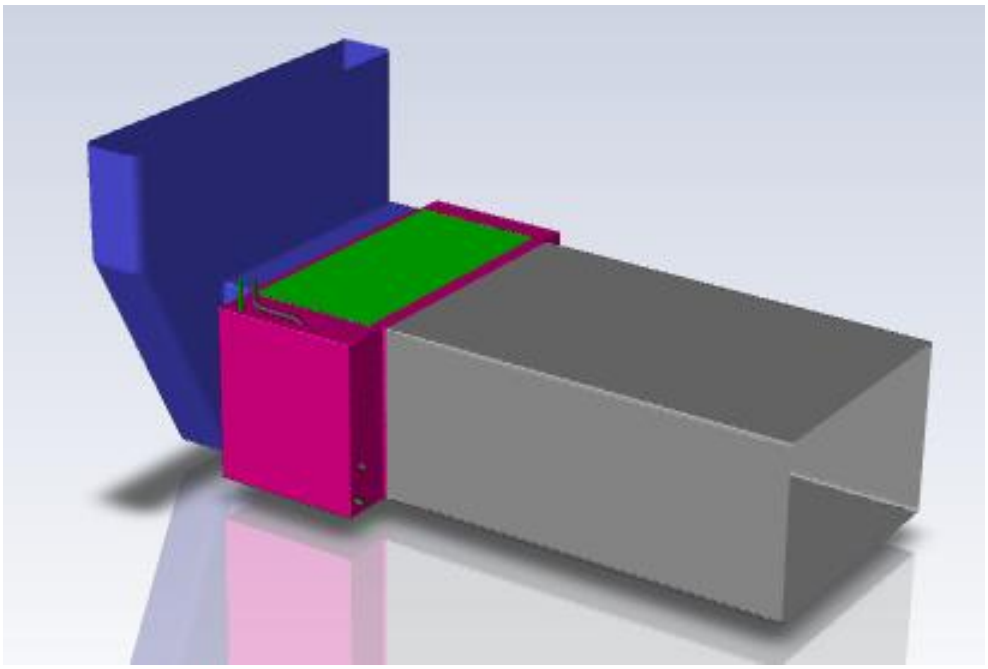

Figure 3. Solution domain

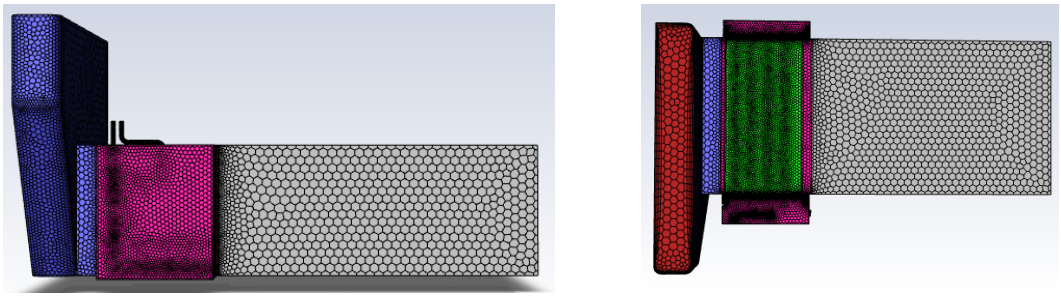

Figure 4. Mesh visual from front and top view

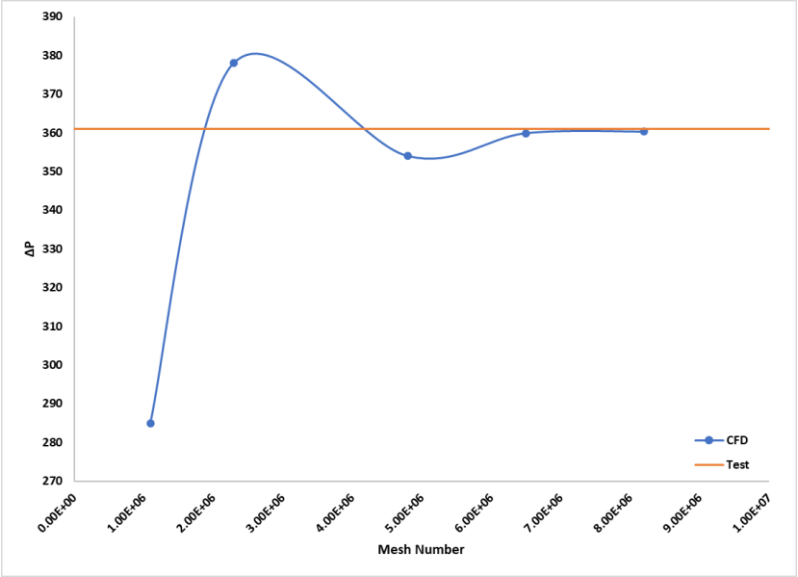

Figure 5. Mesh ındependency

For air flow side, air assumed as dry air and ideal gas assumption were used. For refrigerant side, due to the complexity of multi-phased analysis, water was used instead of refrigerant. Two cases were conducted under same input and boundary conditions which is shown at Figure 6.

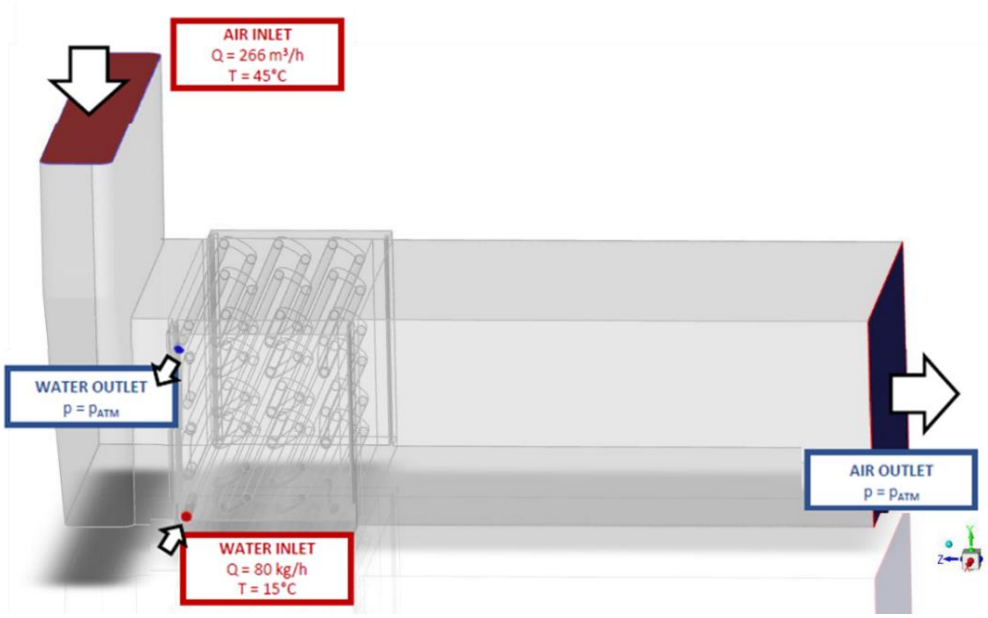

Figure 6. Inputs and boundary conditions

The flow of water and air are turbulent, therefore k- ω SST turbulence model (Menter,1993) was used. Equations of turbulence model is shared in below.

$$\rho\frac{\partial k}{\partial t}+\rho u_i\frac{\partial k}{\partial x_j}=P-\ \beta^*\rho k\omega+\frac{\partial}{\partial x_j}\left[(\mu+\sigma_k\mu_T)\frac{\partial k}{\partial x_j}\right] \quad [1]$$

$$\rho\frac{\partial \omega}{\partial t}+\rho u_i\frac{\partial \omega}{\partial x_j}=\frac{\gamma\rho}{\mu_T}P-\ \beta\rho\omega^2+\frac{\partial}{\partial x_j}\left[(\mu+\sigma_\omega\mu_T)\frac{\partial \omega}{\partial x_j}\right]+2\rho(1-F_1)\frac{\sigma_{\omega 2}}{\omega}\frac{\partial k}{\partial x_j}\frac{\partial \omega}{\partial x_j} \quad [2]$$

For the solution of velocity-pressure couple Reynolds Averaged Navier-Stokes (RANS) Equations (Wilcox, 1998) were used and shown in below. PISO solution algorithm was used for the solution of velocity-pressure couple.

$$\left(\frac{\partial v_x}{\partial x}+\frac{\partial v_y}{\partial y}+\frac{\partial v_z}{\partial z}\right)=0 \quad [3]$$

$$\rho U\left(\frac{\partial U}{\partial x}+\frac{\partial V}{\partial x}+\frac{\partial W}{\partial x}\right)=-\frac{\partial P}{\partial x}+\mu\left(\frac{\partial^2 U}{\partial x^2}+\frac{\partial^2 U}{\partial y^2}+\frac{\partial^2 U}{\partial z^2}\right)-\mu\left(\frac{\partial\overline{u\prime^2}}{\partial x^2}+\frac{\partial\overline{u\prime v\prime}}{\partial x\partial y}+\frac{\partial\overline{u\prime w\prime}}{\partial x\partial z}\right) \quad [4]$$

$$\rho V\left(\frac{\partial U}{\partial y}+\frac{\partial V}{\partial y}+\frac{\partial W}{\partial y}\right)=-\frac{\partial P}{\partial y}+\mu\left(\frac{\partial^2 V}{\partial x^2}+\frac{\partial^2 V}{\partial y^2}+\frac{\partial^2 V}{\partial z^2}\right)-\mu\left(\frac{\partial\overline{u\prime v\prime}}{\partial x\partial y}+\frac{\partial\overline{v\prime^2}}{\partial y^2}+\frac{\partial\overline{v\prime w\prime}}{\partial y\partial z}\right) \quad [5]$$

$$\rho W\left(\frac{\partial U}{\partial z}+\frac{\partial V}{\partial z}+\frac{\partial W}{\partial z}\right)=-\frac{\partial P}{\partial z}+\mu\left(\frac{\partial^2 W}{\partial x^2}+\frac{\partial^2 W}{\partial y^2}+\frac{\partial^2 W}{\partial z^2}\right)-\mu\left(\frac{\partial\overline{u\prime w\prime}}{\partial x\partial z}+\frac{\partial\overline{v\prime w\prime}}{\partial y\partial z}+\frac{\partial\overline{w\prime^2}}{\partial z^2}\right) \quad [6]$$

$$\rho C_p\left(U\frac{\partial T}{\partial x}+V\frac{\partial T}{\partial y}+W\frac{\partial T}{\partial z}\right)=k\left(\frac{\partial^2 T}{\partial x^2}+\frac{\partial^2 T}{\partial y^2}+\frac{\partial^2 T}{\partial z^2}\right) \quad [7]$$

Experimental Phase

After the design and numerical studies, prototype phase was started. Then, two configurations have been assembled one with the current evaporator and the other one with the new evaporator. Two different tests were conducted. One test can be called as temperature difference test which is not normative, and the only thing can be seen is the temperature deviations with the other reference machines. The second test is normative test and it is conducted according to IEC 61121 – Tumble Dryers for Household Use-Methods for Measuring the Performance Standard.

Results and Discussion

Results of Simulation

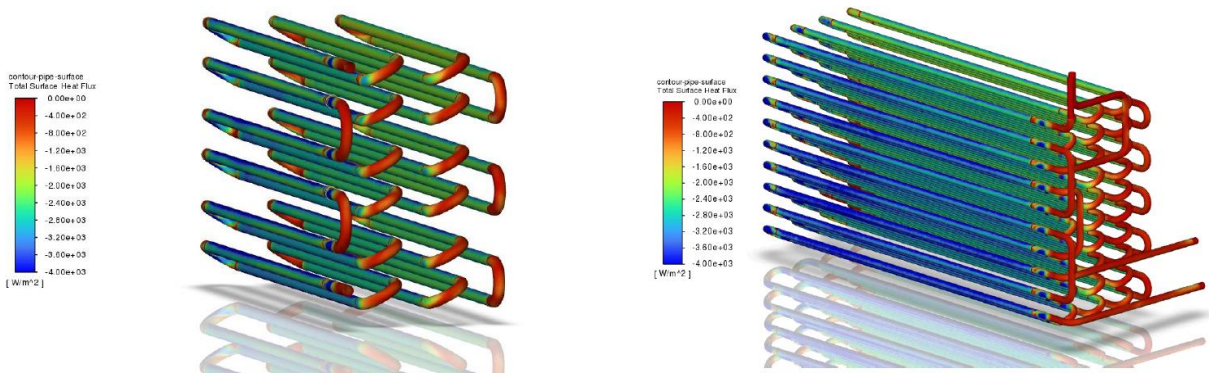

(a) (b)

Figure 7. Heat flux contour of the pipes a) Current b) New evaporator.

The simulations show that new design has an improvement not only for the heat exchange but also flow dynamics. Due to the higher pipe numbers of new design more uniform flow at the evaporator has achieved. Also, heat exchange amount of the evaporator is increased. Figure 7 indicates that with new pipe the system has supplied high heat fluxes for higher surface area even if the maximum flux is not changed. Due to the higher contact surface, outlet temperature of the evaporator is increased. It can be seen at Figure 8.

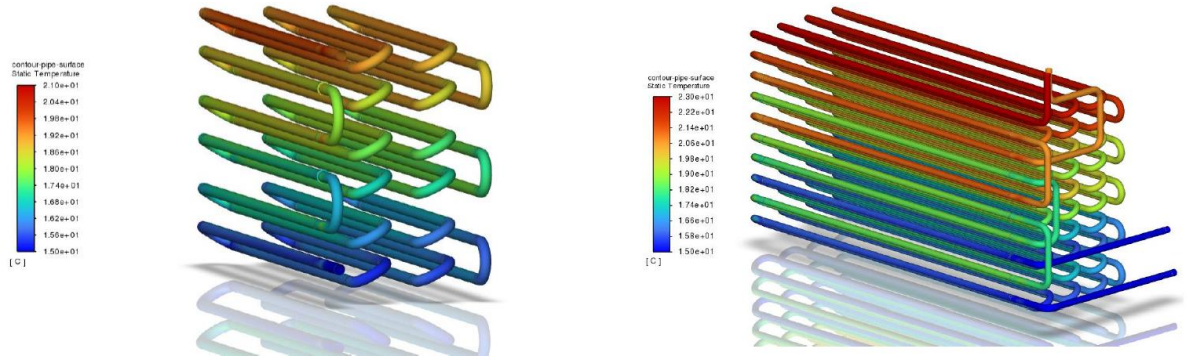

(a) (b)

Figure 8. Temperature contour of the pipes a) Current b) New evaporator.

For the air side, at the entrance no essential difference has been observed. It is due to that; the entrance region of the flow did not be changed. Figure 9 shows the velocity distribution on the evaporator inlet region.

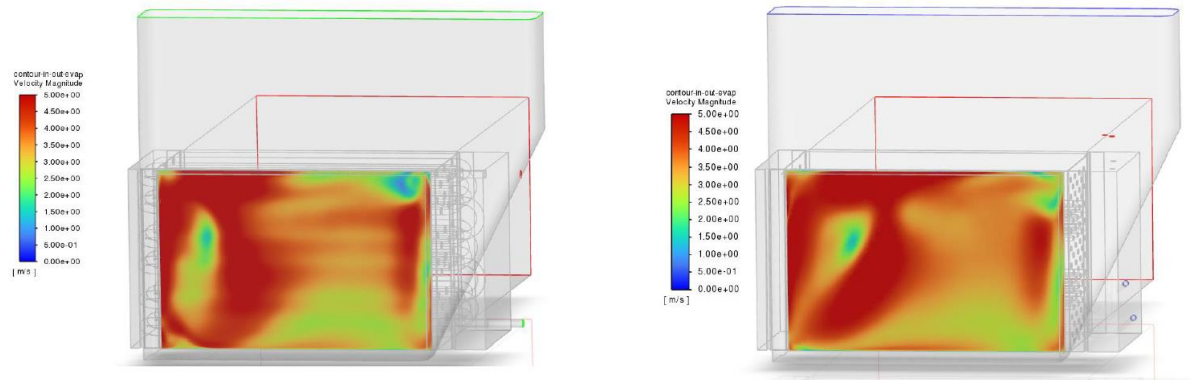

(a) (b)

Figure 8. Velocity distribution contour on the evaporator ınlet a) Current b) New evaporator.

However, due to the higher contact surface lower outlet velocities has achieved, but more uniform velocity distribution is achieved. Figure 9 shows the velocity distribution on the evaporator outlet region.

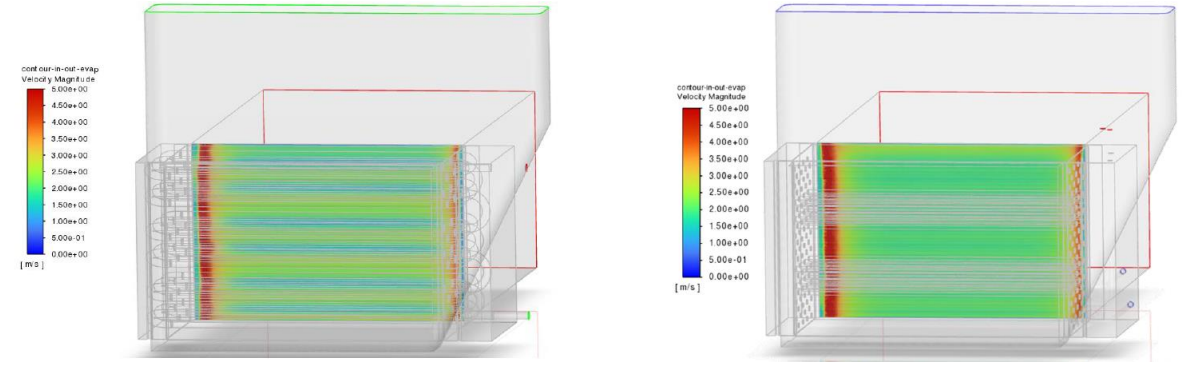

(a) (b)

Figure 9. Velocity distribution contour on the evaporator outlet a) Current b) New evaporator.

The uniformity analysis for the flow side has been conducted and the average velocity values taken from three different planes as following, inlet, middle, outlet. Also, every plane has splitted into four different equal

regions to understand which of the area receive more flow than the others. Figure 10 shows four different regions which velocity values are taken.

Figure 10. Velocity distribution regions

The results show that, with new evaporator the system can receive more uniform airflow then the current one. Results can be seen at Table 1 and also histogram values is shared in Figure 11.

Table 1. Velocity distribution inside the evaporator

Plane	Region	Current Production (m/s)	Percentage of Current Production	New Evaporator (m/s)	Percentage of New Evaporator
Inlet	Top-Left	0.018812	23.9%	0.019424	24.9%
	Top-Right	0.018996	24.2%	0.019606	25.1%
	Bottom-Left	0.020061	25.5%	0.019452	25%
	Bottom-Right	0.020731	26.4%	0.019479	25%
Middle	Top-Left	0.018446	24.4%	0.019397	24.9%
	Top-Right	0.018536	24.5%	0.019775	25.3%
	Bottom-Left	0.019074	25.2%	0.019346	24.8%
	Bottom-Right	0.019512	25.8%	0.019511	25%
Outlet	Top-Left	0.018442	24.3%	0.019346	24.8%
	Top-Right	0.018251	24%	0.019729	25.3%
	Bottom-Left	0.019536	25.7%	0.019325	24.8%
	Bottom-Right	0.019680	25.9%	0.019511	25%

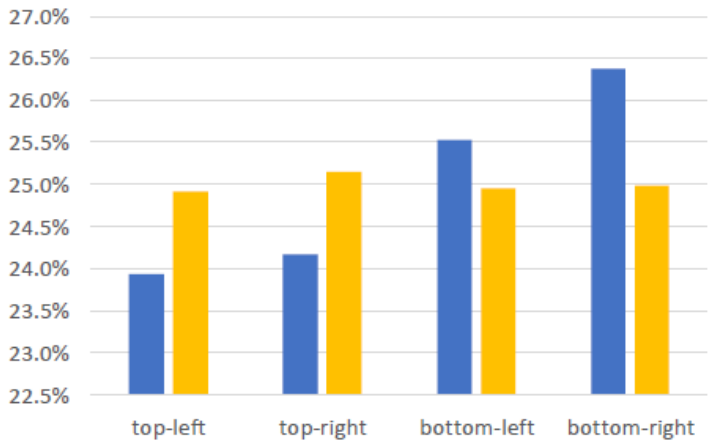

Figure 11. Average velocity distribution on the regions

On the thermal side, new evaporator has 60% increase on the temperature difference on the air side and the total heat exchange is increased 63.4%. In Table 2 summary of the thermal measurements is shared.

Table 2. Summary of the thermal measurements

Cycle	Measurement	Unit	Current Evaporator	New Evaporator
Air Cycle	Mass Flow	kg/h	296.1	296.1
	Avearage T Inlet	°C	45.0	45.0
	Average T Outlet	°C	40.2	37.3
	ΔT	°C	4.8	7.7
	Pipe Surface External	m²	0.0359	0.0484
	Pipe Surface Internal	m²	0.1510	0.2604
	Total Pipe Surface	m²	0.1868	0.3087
	Q Pipe External	W	51.9	47.4
	Q Pipe Internal	W	339.5	592
	Q Pipe Total	W	391.4	639.4
Water Cycle	Mass Flow	kg/h	80.0	80.0
	Avearage T Inlet	°C	15.0	15.0
	Average T Outlet	°C	19.2	21.9
	ΔT	°C	4.2	6.9

Result of Experiments

After the convincing results phase of the simulations, prototype was started and the test that was mentioned in the method section. First test was conducted under same ambient conditions (25°C, 55% r.h.) in this test, two prototypes were built and the only different thing in these prototypes are evaporators. Then, compressor supplied with the electricity and heating on condenser and cooling on the evaporator is observed for 100s. Thermocouples or infrared temperature measurement devices fixed to their positions and tests conducted, respectively. The results show that with new evaporator all system temperatures go down due to the higher capacity of the new evaporator, the comparison results shared in the Figure 12.

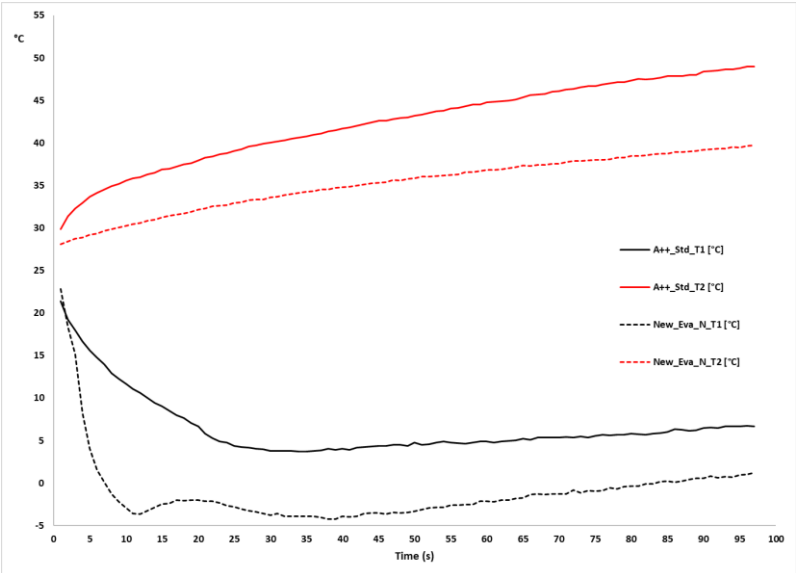

Figure 12. Comparison of temperatures on the evaporator and condenser

After short temperature comparison test, complete machines were built, and tests are conducted according to IEC 61121 standard. Three full load and four half load tests were conducted as stated in standard. Results of one full load and one half load test is shared in Figure 13. On the tests three temperature measurements are taken. T1 temperature on the air temperature and placed between evaporator exit and condenser inlet. T2 Placed at the drum outlet where the air takes humidity from wet clothes. T3 placed on the blowing pipe of the compressor. All temperature measurement shows that with new evaporator all system temperature goes down due to the increased evaporator capacity. However, due to the condenser capacity and compressor capacity remained same the system could not take the humidity from machines and eventually total drying time is elongated with the higher energy consumption. However, these tests indicates that with higher condenser capacity or with the optimized cycle this evaporator can reduce the cycle and/or energy consumption.

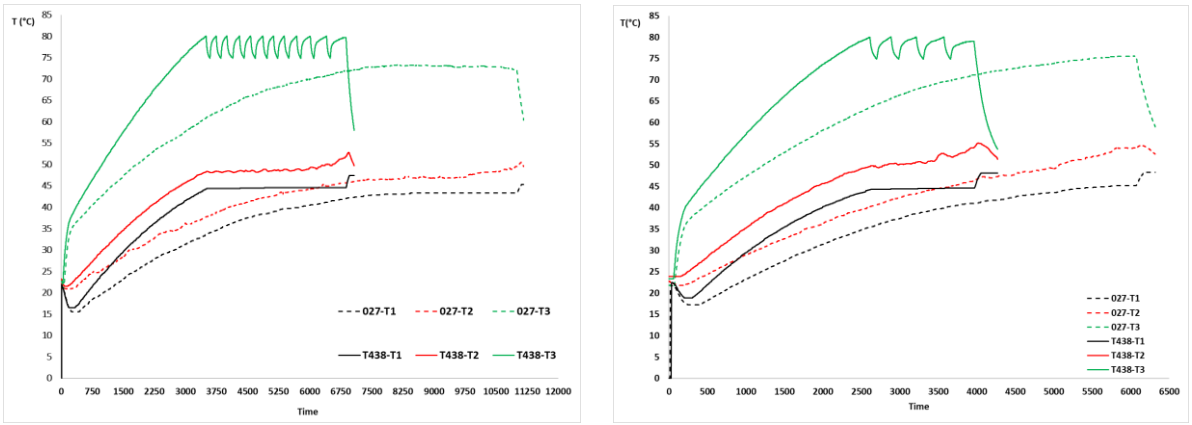

(a) (b)

Figure 13. Temperature comparison on the IEC 61121 test. a) Full load b) Half load

Conclusion

It can be clearly said, the new evaporator has higher capacity from the current one. However, without calibrated or optimized system, our current system could not supply the evaporator well enough. Study also shows that splitting the flow creates a chance to increasing the pipe number and therefore increased exchanger capacity, also with new evaporator more uniformed air flow can be attained. Further research on the evaporator, such as coating the fins with a specific feature, is ongoing. In addition, on the condenser side, a study is ongoing to increase the capacity of the same volume as the current condenser.

Scientific Ethics Declaration

The authors declare that the scientific ethical and legal responsibility of this article published in EPSTEM journal belongs to the authors.

Acknowledgements or Notes

* This article was presented as an oral presentation at the International Conference on Technology, Engineering and Science (www.icontes.net) held in Antalya/Turkey on November 16-19, 2023.

*We extend our gratitude to Renta Electric Home Appliances Industry and Foreign Trade Ltd. and our affiliated company, Haier Europe, for their contributions to our work.

References

IEC 61121(2002). *Tumble dryers for household use-methods for measuring the performance* (3r ed.). Webstore.

Lee, K. S., Jhee, S., & Yang, D. K. (2003). Prediction of the frost formation on a cold flat surface. *International Journal of Heat and Mass Transfer, 46*(20), 3789-3796.

Lenic, K., Trp, A., & Frankovic, B. (2009). Transient two-dimensional model of frost formation on a fin-and-tube heat exchanger. *International Journal of Heat and Mass Transfer*, *52*(1-2), 22-32.

Liu, J., Wei, W., Ding, G., Zhang, C., Fukaya, M., Wang, K., & Inagaki, T. (2004). A general steady state mathematical model for fin-and-tube heat exchanger based on graph theory. *International Journal of Refrigeration, 27*(8), 965-973.

Lu, C. W., Huang, J. M., Nien, W. C., & Wang, C. C. (2011). A numerical investigation of the geometric effects on the performance of plate finned-tube heat exchanger. *Energy Conversion and Management*, *52*(3), 1638-1643.

Menter, F. (1993). Zonal two equation kw turbulence models for aerodynamic flows. In *23rd Fluid Dynamics, Plasmadynamics, and Lasers Conference* (p. 2906).

ONeal, D. L., & Tree, D. R. (1984). Measurement of frost growth and density in a parallel plate geometry. *Ashrae Transactions*, *90*(2), 278-290.

Sami, S. M., & Duong, T. (1989). Mass and heat transfer during frost growth. *ASHRAE Transactions, 95*, 158-165.

Siddique, M., & Alhazmy, M. (2008). Experimental study of turbulent single-phase flow and heat transfer inside a micro-finned tube. *International Journal of Refrigeration, 31*(2), 234-241.

Välikangas, T., & Karvinen, R. (2018). Conjugated heat transfer simulation of a fin-and-tube heat exchanger. *Heat Transfer Engineering, 39*(13-14), 1192-1200.

Wilcox, D. C. (1998). *Turbulence modeling for CFD* (Volume 2, pp. 103-217). La Canada, CA: DCW industries.

Yao, Y., Jiang, Y., Deng, S., & Ma, Z. (2004). A study on the performance of the airside heat exchanger under frosting in an air source heat pump water heater/chiller unit. *International Journal of Heat and Mass Transfer, 47*(17-18), 3745-3756.

Author Information

Fazıl Erinc Yavuz
Haier Europe – Renta Elektrikli Ev Aletleri San ve Dıs Tic. Ltd. Sti
Organize sanayi bolgesi 22. Cadde No: 4
Odunpazarı/Eskisehir Turkiye
Contact e-mail: *erinc.yavuz@haier-europe.com*

Vasıf Can Yildiran
Haier Europe – Renta Elektrikli Ev Aletleri San ve Dıs Tic. Ltd. Sti
Organize sanayi bolgesi 22. Cadde No: 4
Odunpazarı/Eskisehir Turkiye

Sebastian George Colleoni
Haier Europe
Via Privata Eden Fumagalli 20861 Brugherio MB Italy

To cite this article:

Yavuz, F.E., Yildiran, V.C., & Colleoni, S.G. (2023). Examining the performance of the heat exchanger in a heat pump clothes dryer. *The Eurasia Proceedings of Science, Technology, Engineering & Mathematics (EPSTEM), 26*, 156-165.